



THERMAL ANNEALING EFFECTS ON SURFACE MORPHOLOGY AND ELECTRON DYNAMICS IN PSiF-DBT:PCBM BLENDS

Bruno Gabriel Alves Leite Borges¹ , Maiara de Jesus Bassi² , Lucimara Stolz Roman² , Maria Luiza Miranda Rocco^{1*}

1. Universidade Federal do Rio de Janeiro – Instituto de Química – Rio de Janeiro (RJ), Brazil.

2. Universidade Federal do Paraná – Departamento de Física – Curitiba (PR), Brazil.

Corresponding author: luiza@iq.ufrj.br

Section Editor: Mariana Fraga

Received: Mar. 10, 2026 **Approved:** May 17, 2026.

ABSTRACT

We investigated the impact of thermal annealing on the electronic properties, order and transport characteristic of PSiF-DBT:PCBM bulk-heterojunction thin films using sulfur K-edge X-ray absorption spectroscopy (XAS) together with resonant Auger spectroscopy (RAS). PSiF-DBT:PCBM thin films were produced and thermally annealed at two distinct temperatures: 100 and 200°C. RAS experiments, combined with the core-hole clock methodology, were used to extract electron delocalization times by analyzing resonant and normal Auger decay channels following sulfur 1s excitation. The spectroscopic data yield element-specific information on the electronic states of PSiF-DBT and on interfacial charge-transfer processes in PSiF-DBT:PCBM blends as a function of annealing temperature, which was also investigated by atomic force microscopy. This methodology enables direct evaluation of thermal-treatment-induced changes in electronic coupling and charge-transport pathways in silicon-containing donor-acceptor organic semiconductor blends.

KEYWORDS: PSiF-DBT:PCBM, X-ray absorption spectroscopy, Resonant Auger spectroscopy, Electron delocalization, Thermal annealing.

EFEITOS DO RECOZIMENTO TÉRMICO NA MORFOLOGIA DA SUPERFÍCIE E NA DINÂMICA ELETRÔNICA EM MISTURAS DE PSiF-DBT:PCBM

RESUMO

O impacto do recozimento térmico nas propriedades eletrônicas, no ordenamento e nas características de transporte de filmes finos de PSiF-DBT:PCBM foi investigado usando-se espectroscopia de absorção de raios X na borda K do enxofre (XAS) juntamente com espectroscopia Auger ressonante (RAS). Filmes finos de PSiF-DBT:PCBM foram produzidos e tratados termicamente em duas temperaturas distintas: 100 e 200°C. Experimentos de RAS, combinados com a metodologia de *core-hole clock*, foram usados para extrair os tempos de deslocalização eletrônica por meio da análise dos canais de decaimento Auger ressonante e normal após a excitação do elétron 1s do enxofre. Os dados espectroscópicos forneceram informações específicas sobre os estados eletrônicos do PSiF-DBT e sobre os processos de transferência de carga interfacial em misturas de PSiF-DBT:PCBM em função da temperatura de recozimento, que também foi investigada por microscopia de força atômica. Essa metodologia permitiu a avaliação direta das alterações induzidas por tratamento térmico no acoplamento eletrônico e nas vias de transporte de carga em misturas de semicondutores orgânicos doadores-aceitadores contendo silício.

PALAVRAS-CHAVE: PSiF-DBT:PCBM, Espectroscopia de absorção de raios X, Espectroscopia Auger ressonante, Deslocalização eletrônica, Recozimento térmico.

INTRODUCTION

Photovoltaic energy has long been a focal point in scientific research. Using solar energy as fuel, it represents an unlimited and environmentally friendly source of energy. Among the diverse array of photovoltaic technologies prevalent nowadays, those employing thin-films of organic polymers as the photoactive layer are particularly noteworthy, due to their potential to yield cost-effective, flexible, and lightweight devices, contrasting favorably with their inorganic counterparts¹⁻⁴. Despite significant advancements in power conversion efficiencies of these devices over the years, there remains ample room for improvement to enable large-scale industrial production⁵⁻⁷.

The efficiency of these organic devices is influenced by various factors such as film preparation techniques (including deposition method, layer thickness, solar cell architecture, and the implementation of thermal annealing), as well as the morphology, electronic structure, molecular orientation, and charge transfer properties of all materials contained within the device⁸⁻¹⁰.

Within the realm of organic compounds relevant for organic electronic and optoelectronic systems, PSiF-DBT is a low bandgap copolymer that integrates silicon into its chemical structure, acting as a bridging atom in the fluorene, and contains benzothiadiazole units nestled amid thiophene rings (Fig. 1). The larger size of silicon atoms compared to carbon helps improving crystallinity and orientation in the C-Si bond, thereby bolstering the performance of the solar cell device in contrast to the C-C bond¹¹. On the other hand, [6,6]-phenyl-C₆₁-butyric acid methyl ester (PCBM) is a high-quality electron acceptor for organic photovoltaics, featuring high electron mobility. Its solubility in common solvents used for donor polymers enables the simultaneous casting of both polymer and fullerene, promoting the formation of an efficient bulk-heterojunction with rapid charge transfer and exciton dissociation¹²⁻¹⁴.

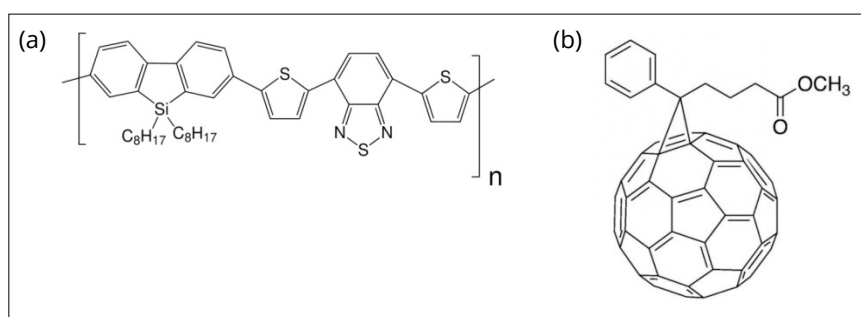


Figure 1: Chemical structure representations of (a) poly[2,7-(9,9-bis(2-ethylhexyl)-dibenzosilole)-alt-4,7-bis(thiophen-2-yl)benzo-2,1,3-thiadiazole] (PSiF-DBT) and (b) [6,6]-phenyl-C₆₁-butyric acid methyl ester (PCBM).

When producing thin films in a bulk-heterojunction configuration, thermal annealing is a pivotal step that can significantly enhance device performance optimizing morphology, reducing defects, enhancing crystallinity, eliminating residual solvents, and by fine-tuning optical properties. Although we have previously reported studies for PSiF-DBT films, PSiF-DBT:PCBM and PSiF-DBT:PC71BM blends^{8,15-17}, the effect of thermal annealing on PSiF-DBT:PCBM blends have not been discussed yet.

To assess the impact of thermal annealing on the electronic properties, order, and transport characteristics of PSiF-DBT:PCBM films, we analyzed the samples through X-ray absorption spectroscopy (XAS) and resonant Auger spectroscopy (RAS).

XAS is an analytical technique used to investigate the electronic states of specific elements within a material. When X-rays are directed at a sample, they can be absorbed by the atoms, causing the ejection of electrons from their inner shells. This absorption process provides information about the electronic structure and chemical environment of the element^{18,19}.

On the other hand, RAS is valuable in probing charge transfer mechanisms by measuring decay channels from the core excited state using the core-hole clock (CHC) method. This method leverages core-hole decay as an internal clock for the Auger decay process. Detailed explanations are available in other studies^{20,21}.

Briefly, the observation of normal Auger decay peak in the RAS spectrum when using an incident photon at the resonant energy of the photoabsorption spectrum indicates that the photoexcited electron transfers into the surface or surroundings before the core-hole decay relaxation process, and so the electron delocalization time can be probed.

In this work, our aim was to investigate the impact of thermal annealing on both electron delocalization times, accessed via the CHC method, and the morphology of PSiF-DBT:PCBM blends treated at various temperatures.

MATERIALS AND METHODS

Preparation of PSiF-DBT:PCBM thin films

The blend in a 1:3 weight rate of PSiF-DBT:PCBM was spin coated onto pre-cleaned patterned indium tin oxide coated glass substrates under nitrogen atmosphere from 18 mg/mL dichlorobenzene solution. Other two blended films were obtained by 15 minutes of thermal annealing treatments at 100 and 200°C in vacuum. Film thickness of 70 nm was measured using Dektak 150 profilometer (Veeco Instruments).

Measurements

The ultraviolet-visible spectra were obtained by a Shimadzu spectrophotometer model NIR 2101. Fluorog[®] - 3 spectrofluorometer equipment was used for photoluminescence measurements.

Atomic force microscopy measurements were also performed. The operating mode of the microscope used was intermittent contact through the Shimadzu microscope, model SPM-9700.

S-K edge XAS and RAS were acquired at the Brazilian Synchrotron Light Laboratory in the total electron yield detection mode. Detailed information regarding the experimental setup can be found in Borges et al.²¹. The linear dichroism of all films was further examined by varying the angle between the incident radiation and the substrate.

Auger decay spectra were carried out by using a hemispherical electron energy analyzer employing a pass energy of 20 eV. For curve fitting analysis of the resonant Auger spectra, a linear combination of Gaussian (G) and Lorentzian (L) peak shape functions was used through the licensed CasaXPS software.

RESULTS AND DISCUSSION

Optical characterization of PSiF-DBT and PSiF-DBT:PCBM films

Ultraviolet-visible absorption and photoluminescence (PL) measurements were performed to investigate the optical properties and donor-acceptor interactions in pristine PSiF-DBT and PSiF-DBT:PCBM blend films (Fig. 2a). The absorption spectrum of pristine PSiF-DBT exhibits two distinct bands. The higher-energy band, located in the near-ultraviolet region, is attributed to localized π - π^* transitions along the conjugated backbone. The lower-energy and broader band extending into the visible region is assigned to an intramolecular charge-transfer transition between the electron-rich thiophene/fluorene units and the electron-deficient benzothiadiazole moieties. This dual-band feature is characteristic of donor-acceptor copolymers and reflects the reduced optical bandgap of PSiF-DBT²².

Upon blending with PCBM, the overall spectral profile of the polymer is largely preserved, indicating that the ground-state electronic structure of PSiF-DBT remains essentially unchanged in the bulk-heterojunction configuration. The preservation of the characteristic absorption bands suggests that no significant chemical modification occurs upon fullerene incorporation.

However, a pronounced quenching of the PL is observed in the PSiF-DBT:PCBM blend compared to the pristine polymer film (Fig. 2b). This strong PL quenching indicates efficient exciton dissociation and photoinduced charge transfer at the donor–acceptor interface, confirming the effective electronic coupling between PSiF-DBT and PCBM in the bulk-heterojunction system²³. The observed quenching behavior is consistent with the charge-transfer dynamics later probed by RAS, reinforcing the role of interfacial electronic interactions in these blends.

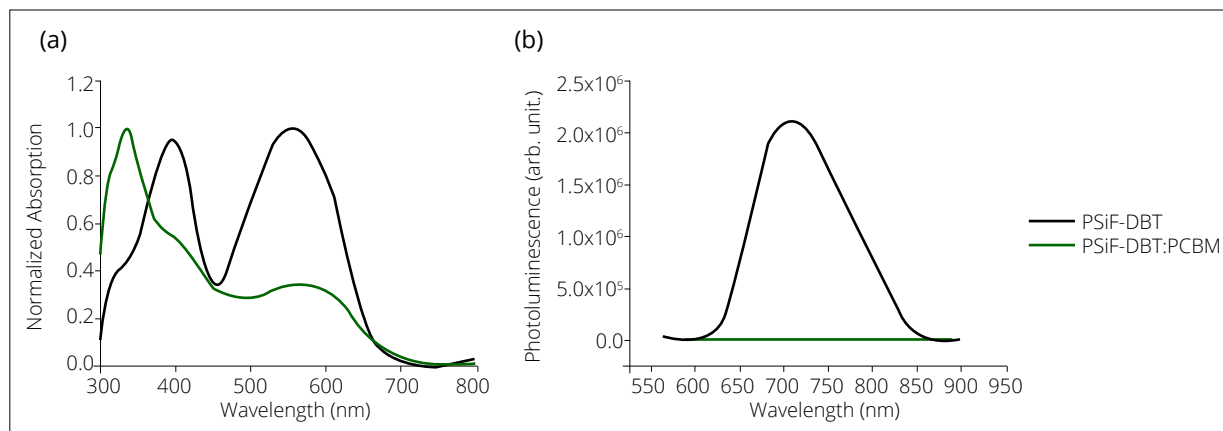


Figure 2: (a) Normalized ultraviolet–visible absorption spectra of pristine PSiF-DBT and PSiF-DBT:PCBM blend films. (b) Photoluminescence spectra of the corresponding films, showing strong photoluminescence quenching in the blend, indicative of efficient exciton dissociation and interfacial charge transfer in the bulk-heterojunction system.

X-ray absorption spectra

Figure 3 shows the angular-dependent S1s X-ray absorption spectra (XAS) of PSiF-DBT:PCBM samples measured at different annealing temperatures: as-cast (left), 100°C (middle), and 200°C (right). Across all samples, four well-defined spectral features are observed in the S1s XAS spectra in the region between 2,470 and 2,476 eV. Inspection of the PSiF-DBT chemical structure revealed the presence of two distinct sulfur chemical environments: one associated with the electron-rich thiophene unit, and the other with the electron-deficient benzothiadiazole unit. This interpretation is consistent with previous reports by Aygül et al.²⁴, as well as with our earlier studies on PSiF-DBT films^{15–17}. The spectral features labeled B1 and B2 are assigned respectively to the S 1s → π^* and S 1s → σ^* (S–N) transitions, originating from sulfur atoms within the benzothiadiazole units. In contrast, the T1 and T2 features correspond to the S 1s → π^* and S 1s → σ^* (S–C) transitions associated with sulfur atoms in the thiophene units. Previous studies have reported a preferential edge-on orientation for thiophene units and a face-on (plane-on) orientation for benzothiadiazole units, providing a structural framework for interpreting the observed angular dependence in the XAS spectra¹⁶. N1s XAS spectra for the benzothiadiazole units in PSiF-DBT:PC71BM films also corroborate a face-on (plane-on) orientation¹⁵.

The XAS spectra of all samples show a clear angular dependence, reflecting changes in the orientation and ordering of the sulfur-containing units within the PSiF-DBT backbone. These are very similar to PSiF-DBT XAS data obtained in our previous work, since the presence of PCBM does not change the sulfur environment¹⁶.

For the as-cast sample, T1 transition reaches maximum intensity under normal incidence, whereas the T2 peak is more pronounced at grazing incidence. In contrast, the B1 and B2 features show higher intensity at grazing incidence and are attenuated under normal incidence. Upon thermal annealing, the dichroism observed in XAS spectra of all four transitions is somehow enhanced. The distinct dichroic responses of the B- and T-related features further suggest that benzothiadiazole and thiophene units respond differently upon annealing, consistent with their different electronic character and preferred geometries.

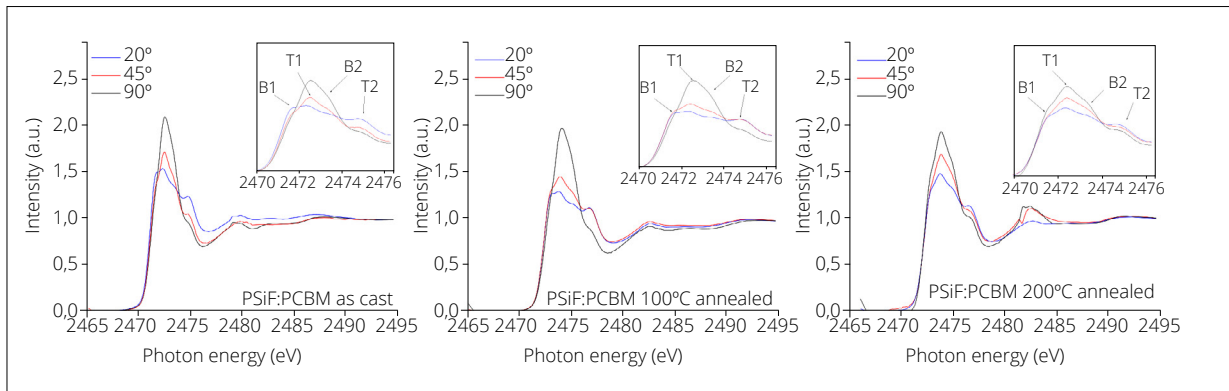


Figure 3: Angular-dependent S1s X-ray absorption spectra of PSiF-DBT:PCBM blends (as-cast and annealed at 100 and 200°C).

Resonant Auger spectra

Figure 4 presents the $S\text{KL}_{2,3}\text{L}_{2,3}$ RAS of all PSiF-DBT:PCBM films (as-cast and annealed at 100 and 200°C), recorded at selected incident photon energies corresponding to the B1 (2471.8 eV), T1 (2472.6 eV), B2 (2473.3 eV) and T2 (2474.4 eV) resonances identified in the corresponding XAS spectra from Fig. 3.

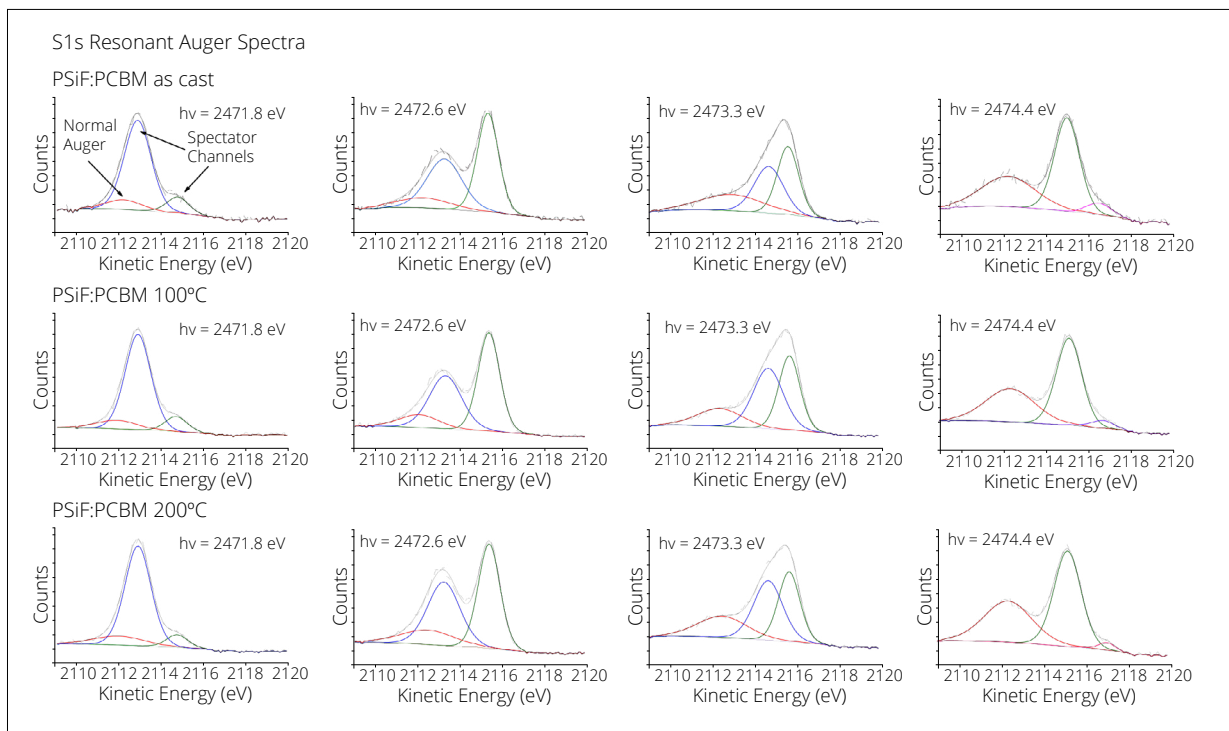


Figure 4: $S\text{KL}_{2,3}\text{L}_{2,3}$ resonant Auger results for PSiF-DBT:PCBM blends (as-cast, and annealed at 100 and 200°C).

As reported for PSiF-DBT^{16,17}, the RAS spectra recorded exhibit three distinct decay channels: a normal Auger decay centered at 2,112 eV, and two spectator decay features associated with $S1s \rightarrow \pi^*$ and $S1s \rightarrow \sigma^*$ transitions, appearing at progressively higher kinetic energies. To identify the parameters for the normal Auger decay feature, we have used the Auger spectrum measured above S1s ionization potential. The full procedure to identify and fit these peaks was previously reported by Garcia-Basabe et al.^{16,17}. Charge-transfer times (τ_{CT}) were derived using a sulfur 1s core-hole lifetime of 1.27 fs²⁵, together with the core-hole clock formalism described in previous works^{17,20,21,26–28}. Table 1 summarizes the resulting τ_{CT} values.

B1 and T1 resonant energies yield similar charge-transfer times for the as-cast and 100°C annealed PSiF-DBT:PCBM films. The differences in τ_{CT} values are 0.1 fs for the B1 transition and 0.5 fs for the T1 transition. In contrast, the 200°C annealed blend exhibits the fastest charge-transfer dynamics, with τ_{CT} values approximately 2 fs shorter. This demonstrates the importance of thermal annealing in improving nanoscale organization and interfacial charge transport in donor-acceptor blends, which is also consistent with an enhanced film morphology, as shown by the photoabsorption results.

At the remaining energies, the values are comparable, except for the blend annealed at 100°C, which shows a slower charge-transfer time (5.4 fs). This behavior is expected because the energy values lie close to the ionization potential.

Table 1: Derived charge transfer times (τ_{CT}) using the core-hole clock method for PSiF-DBT:PCBM blends (as-cast, and annealed at 100 and 200°C).

Sample	h ν =2,471.8 eV (B1)	h ν = 2,472.6 eV(T1)	h ν = 2,473.3 eV(B2)	h ν = 2,474.4 eV(T2)
PSiF:PCBM as-cast	τ_{CT} = 10.3 fs	τ_{CT} = 9.2 fs	τ_{CT} = 3.6 fs	τ_{CT} = 2.0 fs
PSiF:PCBM 100°C annealed	τ_{CT} = 10.2 fs	τ_{CT} = 9.7 fs	τ_{CT} = 5.4 fs	τ_{CT} = 1.4 fs
PSiF:PCBM 200°C annealed	τ_{CT} = 8.1 fs	τ_{CT} = 7.0 fs	τ_{CT} = 3.9 fs	τ_{CT} = 1.7 fs

Morphological evolution upon thermal annealing

Atomic force microscopy was employed to investigate the morphological changes induced by thermal annealing in PSiF-DBT:PCBM films. As shown in Fig. 5, the as-cast film exhibits a relatively smooth surface, characteristic of a finely intermixed bulk-heterojunction morphology.

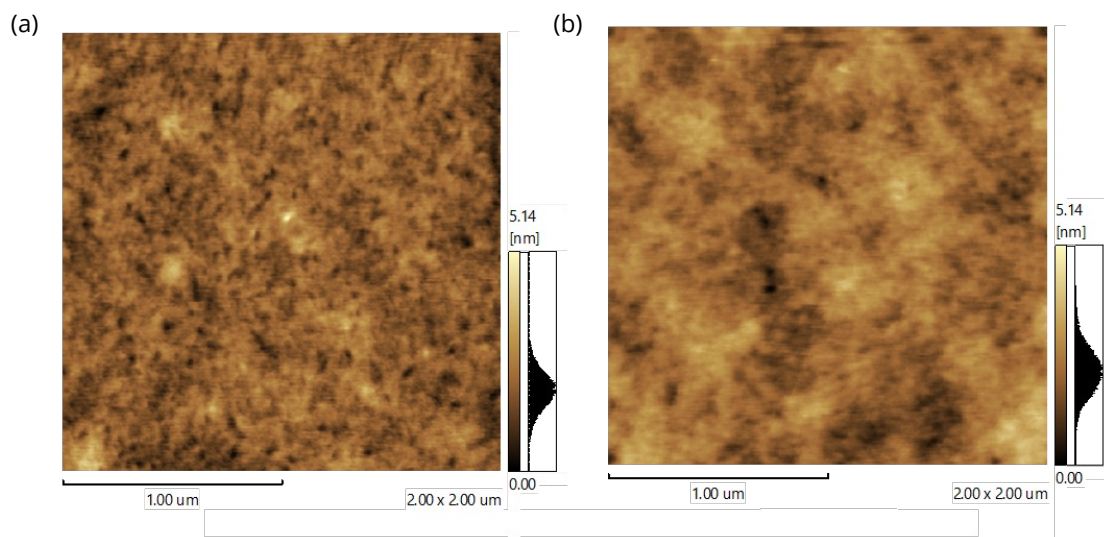


Figure 5: Atomic force microscopy topographic images ($2 \times 2 \mu\text{m}^2$) of PSiF-DBT:PCBM films: (a) as-cast and (b) annealed at 200°C. Thermal treatment leads to a ~13% increase in root-mean-square surface roughness, suggesting enhanced nanoscale reorganization and phase segregation in the blend.

After annealing at 200°C, the film displays a moderate increase in RMS roughness of 13%. This increase in surface roughness suggests thermally induced reorganization and enhanced phase segregation at the nanoscale. Such morphological evolution is commonly associated with improved donor-acceptor domain definition and enhanced interfacial area, which can facilitate exciton dissociation and charge transport. The improved nanoscale organization is consistent with the shorter charge-transfer times observed in the 200°C annealed film, as revealed by the core-hole clock analysis⁷.

CONCLUSION

Sulfur K-edge XAS and RAS were used to probe the effects of thermal annealing on the molecular orientation and charge-transfer dynamics in PSiF-DBT:PCBM bulk-heterojunction films. The RAS spectra exhibit a normal Auger decay at around 2,112 eV and spectator Auger decays associated with $S\ 1s \rightarrow \pi^*$ and σ^* excitations, consistent with previous reports for PSiF-DBT systems.

Charge-transfer times extracted using the core-hole clock formalism showed similar dynamics for as-cast and 100°C annealed films at the B1 and T1 resonances, while the blend annealed at 200°C displayed significantly faster charge transfer, with τ_{CT} values approximately 2 fs shorter. At higher excitation energies, τ_{CT} values were comparable among samples, except for the 100°C annealed film.

Angle-dependent XAS measurements displayed an overall increase in dichroism after annealing, indicating improved molecular ordering. These results show that thermal annealing strongly influences molecular organization and ultrafast interfacial charge-transfer processes in PSiF-DBT:PCBM blends. The modification of molecular organization upon annealing were verified by atomic force microscopy measurements on the surface of the films.

CONFLICT OF INTEREST

Nothing to declare.

AUTHOR CONTRIBUTIONS


Conceptualization: Roman LS and Rocco MLM; **Formal Analysis:** Borges BGAL and Bassi MJ; **Investigation:** Borges BGAL, Bassi MJ and Rocco MLM; **Resources:** Roman LS and Rocco MLM; **Supervision:** Roman LS and Rocco MLM; **Validation:** Roman LS and Rocco MLM; **Data curation:** Roman LS and Rocco MLM; **Writing – original draft:** Borges BGAL, Bassi MJ; **Writing – review and editing:** Roman LS and Rocco MLM; **Final approval:** Roman LS and Rocco MLM.


AVAILABILITY OF DATA AND MATERIALS

The data will be available upon request.

FUNDING

Conselho Nacional de Desenvolvimento Científico e Tecnológico 
Grant No.: 306565/2025-0

Fundação Carlos Chagas Filho de Amparo à Pesquisa do Estado do Rio de Janeiro 
Grant No.: E-26/210.108/2023

Laboratório Nacional de Luz Síncrotron 
Grant No.: Proposal 20180092



DECLARATION OF USE OF INTELLIGENCE ARTIFICIAL TOOLS

Artificial intelligence tools were not used.

ACKNOWLEDGEMENTS

Not applicable.

REFERENCES

1. Sun Y, Wang L, Guo C, Xiao J, Liu C, Chen C, Xia W, Gan Z, Cheng J, Zhou J, Chen Z, Zhou J, Liu D, Wang T, Li W. π -extended nonfullerene acceptor for compressed molecular packing in organic solar cells to achieve over 20% efficiency. *J Am Chem Soc.* 2024;146(17):12011-9. <https://doi.org/10.1021/jacs.4c01503>
2. Rafique S, Abdullah SM, Sulaiman K, Iwamoto M. Fundamentals of bulk heterojunction organic solar cells: an overview of stability/degradation issues and strategies for improvement. *Renew Sustain Energy Rev.* 2018;84:43-53. <https://doi.org/10.1016/j.rser.2017.12.008>
3. Kumar S, Sharma A, Pathak D, Nunzi JM. Bulk heterojunction solar cells. In: Kumar V, Pathak D, Sharma DP, Nunzi JM, editors. *Solar Cell Engineering: advanced materials and technologies for photovoltaics.* Elsevier; 2026. p. 203-28. <https://doi.org/10.1016/B978-0-443-29250-7.00012-8>
4. Bassi MDJ, Benatto L, Wouk L, Holakoei S, Oliveira CK, Rocco MLM, Roman LS. Correlation between structural and optical characteristics of conjugated copolymers differing by a Si bridge atom. *Phys Chem Chem Phys.* 2020;22(35):19923-31. <https://doi.org/10.1039/D0CP02520H>
5. He Y, Li N, Heumüller T, Wortmann J, Hanisch B, Aubele A, Lucas S, Feng G, Jiang X, Li W, Bäuerle P, Brabec CJ. Industrial viability of single-component organic solar cells. *Joule.* 2022;6(6):1160-71. <https://doi.org/10.1016/j.joule.2022.05.008>
6. Majhi J, Ghosh S, Priya K, Sharma S, Bandyopadhyay A. A critical review on the progress of emerging active and substrate materials for organic solar cells and device level fabrication techniques by solution process method. *Next Mater.* 2025;8:100595. <https://doi.org/10.1016/j.nxmater.2025.100595>
7. Marchiori CFN, Yamamoto NAD, Matos CF, Kujala J, Macedo AG, Tuomisto F, Zarbin AJG, Koehler M, Roman LS. Annealing effect on donor-acceptor interface and its impact on the performance of organic photovoltaic devices based on PSiF-DBT copolymer and C60. *Appl Phys Lett.* 2015;106:133301. <https://doi.org/10.1063/1.4916515>
8. Marchiori CFN, Garcia-Basabe Y, de A Ribeiro F, Koehler M, Roman LS, Rocco MLM. Thermally induced anchoring of fullerene in copolymers with Si-bridging atom: Spectroscopic evidences. *Spectrochim Acta A Mol Biomol Spectrosc.* 2017;171:376-82. <https://doi.org/10.1016/j.saa.2016.08.010>
9. Zhou H, Yang L, You W. Rational design of high performance conjugated polymers for organic solar cells. *Macromolecules.* 2012;45(2):607-32. <https://doi.org/10.1021/ma201648t>
10. Bulavko G. Organic photovoltaics: A journey through time, advancements, and future opportunities. *Hist Sci Technol.* 2024;14(1):10-32. <https://doi.org/10.32703/2415-7422-2024-14-1-10-32>
11. Shmakov SN, Jia Y, Pinkhassik E. Selectively initiated ship-in-a-bottle assembly of yolk-shell nanostructures. *Chem Mater.* 2014;26(2):1126-32. <https://doi.org/10.1021/cm403442k>
12. Chen D, Nakahara A, Wei D, Nordlund D, Russell TP. P3HT/PCBM bulk heterojunction organic photovoltaics: correlating efficiency and morphology. *Nano Lett.* 2011;11(2):561-7. <https://doi.org/10.1021/nl103482n>
13. Sahoo S, Barah D, Kumar SD, Xavier N, Dutta S, Ray D, Bhattacharyya J. The nature of excitons in PPDT2FBT:PCBM solar cells: role played by PCBM. *J Phys D Appl Phys.* 2022;55:455103. <https://doi.org/10.1088/1361-6463/ac8819>

14. Mikroyannidis JA, Kabanakis AN, Sharma SS, Sharma GD. A simple and effective modification of PCBM for use as an electron acceptor in efficient bulk heterojunction solar cells. *Adv Funct Mater.* 2011;21(4):746-55. <https://doi.org/10.1002/adfm.201001807>
15. Marchiori CFN, Garcia-Basabe Y, Matos CF, Koehler M, Roman LS, Rocco MLM. Thermal annealing effects on the morphology and electronic structure of PSiF-DBT:PCBM thin films. *Thin Solid Films.* 2016;618:150-6.
16. Garcia-Basabe Y, Marchiori CFN, Borges BGAL, Yamamoto NAD, Macedo AG, Koehler M, Roman LS, Rocco MLM. Electronic structure, molecular orientation, charge transfer dynamics and solar cell performance in donor/acceptor copolymers and fullerene: experimental and theoretical approaches. *J Appl Phys.* 2014;115:134901. <https://doi.org/10.1063/1.4870470>
17. Garcia-Basabe Y, Marchiori CFN, Moura CEV, Rocha AB, Roman LS, Rocco MLM. Charge transfer dynamics and molecular orientation probed by core electron spectroscopies on thermal-annealed polysilafluorene derivative: experimental and theoretical approaches. *J Phys Chem C.* 2014;118(41):23863-73. <https://doi.org/10.1021/jp508010u>
18. Ishikawa D. Recent topics in X-ray absorption spectroscopy: integrating theory, instrumentation, and applications. *Anal Sci.* 2025;41(10):1573-4. <https://doi.org/10.1007/s44211-025-00840-7>
19. Yano J, Yachandra VK. X-ray absorption spectroscopy. *Photosynth Res.* 2009;102(2-3):241-54. <https://doi.org/10.1007/s11120-009-9473-8>
20. Menzel D. Ultrafast charge transfer at surfaces accessed by core electron spectroscopies. *Chem Soc Rev.* 2008;37(10):2212-23. <https://doi.org/10.1039/B719546j>
21. Borges BGAL, Roman LS, Rocco MLM. Femtosecond and attosecond electron transfer dynamics of semiconductors probed by the core-hole clock spectroscopy. *Top Catal.* 2019;62:1004-10. <https://doi.org/10.1007/s11244-019-01189-8>
22. Bassi MDJ, Benatto L, Wouk L, Holakoei S, Oliveira CK, Rocco MLM, Roman LS. Correlation between structural and optical characteristics of conjugated copolymers differing by a Si bridge atom. *Phys Chem Chem Phys.* 2020;22(35):19923-31. <https://doi.org/10.1039/D0CP02520H>
23. Benatto L, Moraes CAM, Bassi MJ, Wouk L, Roman LS, Koehler M. Kinetic modeling of the electric field dependent exciton quenching at the donor-acceptor interface. *J Phys Chem C.* 2021;125(8):4436-48. <https://doi.org/10.1021/acs.jpcc.0c11458>
24. Aygül U, Batchelor D, Dettinger U, Yilmaz S, Allard S, Scherf U, Peisert H, Chassé T. Molecular orientation in polymer films for organic solar cells studied by NEXAFS. *J Phys Chem C.* 2012;116(7):4870-4. <https://doi.org/10.1021/jp205653n>
25. Campbell JL, Papp T. Widths of the atomic K-N7 levels. *At Data Nucl Data Tables.* 2001;77(1):1-56. <https://doi.org/10.1006/adnd.2000.0848>
26. Garcia-Basabe Y, Borges BGAL, Silva DC, Macedo AG, Micaroni L, Roman LS, Rocco MLM. The interplay of electronic structure, molecular orientation and charge transport in organic semiconductors: poly(thiophene) and poly(bithiophene). *Org Electron.* 2013;14(11):2980-6. <https://doi.org/10.1016/j.orgel.2013.08.022>
27. Borges BGAL, Veiga AG, Tzounis L, Laskarakis A, Logothetidis S, Rocco MLM. Molecular orientation and ultrafast charge transfer dynamics studies on the P3HT:PCBM blend. *J Phys Chem C.* 2016;120(43):25078-82. <https://doi.org/10.1021/acs.jpcc.6b08056>
28. Misael WA, Péan EV, Borges BGAL, Mello GC, Wouk L, Davies ML, Roman LS, Rocco MLM. Molecular orientation and femtosecond electron transfer dynamics in halogenated and nonhalogenated, eco-friendly processed PTB7-Th, ITIC, PTB7-Th:ITIC, and PTB7-Th:PCBM films. *J Phys Chem C.* 2022;126(26):10807-17. <https://doi.org/10.1021/acs.jpcc.2c01298>